Geodetic Position Estimation for a Geosynchronous Satellite

N. Nagarajan,* S. Akila,* and S. V. Rao*
ISRO Satellite Centre, Bangalore, India

Introduction

GEOSTATIONARY satellites are subject to various perturbing forces like Earth's triaxiality, solar radiation pressure, and lunisolar attraction. Nevertheless, the satellite is to be maintained within tight longitude and latitude windows. The need to reduce the dependence on ground station has given rise to many autonomous satellite position determination techniques based on measurements like known Earth landmarks, Earth sensors, star sensors, sun sensors, and stellar refraction, etc.[1-4] The main objective is to stationkeep the satellite within the allowed window for which the geodetic coordinates are important. If the state to be estimated is defined as the position in Greenwich frame, then a very simple filter and dynamics model can be used to estimate the state. In the present study, the measurements range from three active landmarks to the candidate satellite. Simulation studies carried out for a nearly geostationary orbit as well as an inclined drift orbit show that the current state (i.e., position in Greenwich frame) can be estimated to an accuracy better than 200 m in each component when the measurements interval is 30 min.

Measurement Equations

Figure 1 shows the configuration chosen for the present study. *BMi* ($i=1,2,3$) are the three active landmarks with their geodetic position known accurately. These landmarks are transceivers that can be activated by a remote signal. The signal originates from the satellite and essentially consists of a time mark. As soon as the activating signal is received, the active landmarks reply back by retransmitting the signal toward the satellite after adding their identification codes. The signal is finally received at the satellite where range is calculated using the time of reception, the time mark, and the coordinates of the active landmark picked up from the library using the identification code.

Let $\bar{S}_i$ ($i=1,2,3$) and $\bar{X}$ be the geodetic position vectors of the active landmarks and the satellite. Then the slant range, ρ_i, is

$$(\bar{X}-\bar{S}_i)^T(\bar{X}-\bar{S}_i)=\rho^2, \qquad i=1,2,3\ldots \tag{1}$$

Error Analysis

The actual measurements represented by Eqs. (1) contain noise and bias errors. Linearizing Eqs. (1) around nominal value yields

$$\Delta\rho=H\cdot\Delta\bar{X}+\nu \tag{2}$$

where H is the 3×3 matrix of measurement partials, and ν is the 3×1 vector of measurement noise. The covariance p of position estimate is

$$P=(H^TH)^{-1}\sigma^2 \tag{3}$$

where σ is standard deviation of the range measurements.

The square root of the trace of $(H^TH)^{-1}$ is defined as the geometric dilution of precision (GDOP). With the set of active landmarks given in Table 1 and the satellite of 80° E long, the GDOP from Eq. (3) is 36, and the diagonal elements of $(H^TH)^{-1}$ are (634, 17, 673). This means that if the range noise is 5 m, then with a single set of measurements the position determination error is around 180 m. With n such measurement sets the GDOP decreases by a factor $\sqrt{n}$.

Filter Equations

Since the Eqs. (1) governing the measurements are nonlinear, the position is estimated by first linearizing Eqs. (1) around the a priori value and then applying the linear Kalman filter. The filter equations are as follows[5]:

Measurement equation

$$y=H\tilde{x}+\nu \tag{4}$$

Predicted state

$$\tilde{x}=\hat{x}+\int\dot{x}\cdot dt \tag{5}$$

Predicted covariance

$$\tilde{P}=\phi\hat{P}\phi^T+Q \tag{6}$$

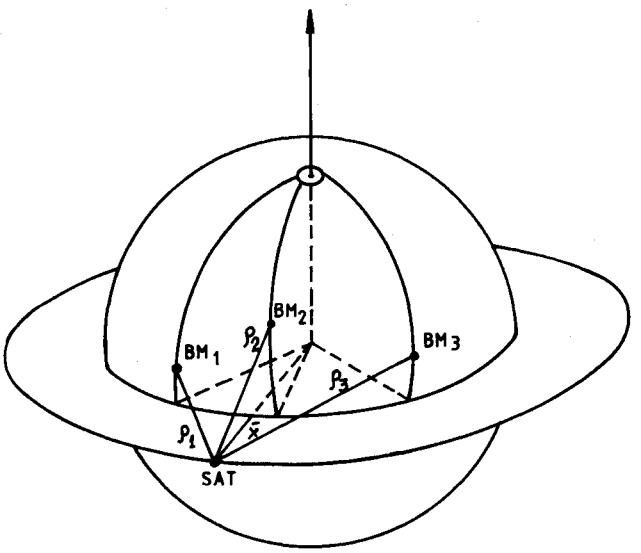

Fig. 1 Satellite: active landmarks' geometry.

Table 1 Simulation Details

State Vector and Epoch

Case 1			Case 2		
X	−11547.0955	kms	X	−11540.1942	kms
Y	40552.4219	kms	Y	40528.0056	kms
Z	0.0	kms	Z	0.0	kms
X	−2.957116	km/s	X	−2.957664	km/s
Y	−0.842027	km/s	Y	−0.842183	km/s
Z	−0.000536	km/s	Z	0.053678	km/s
Epoch date 1987-1-1 Time 19:00:00 hr (UT)			Epoch date 1987-1-1 Time 19:00:00 hr (UT)		

Mass = 650 kg, area = 12.137 m^2, reflectivity = 1.5, Earth potential 24 × 24. Solar radiation pressure and lunisolar forces are considered.

Observation details

Observations: range from three active landmarks to satellite at any instant with a noise of 3 m (1σ) and a bias of 3 m.

Active landmarks' coordinates

Name	Latitude, deg	Longitude, deg
BM1	8 N	78 E
BM2	24 N	72 E
BM3	28 N	94 E

Received Aug. 10, 1987; revision received Aug. 2, 1988.

*Engineer, Flight Dynamics Division.

Kalman gain

$$k = \tilde{P}H^T(H\tilde{P}H^T + R)^{-1} \tag{7}$$

Updated state

$$\hat{x} = \tilde{x} + k(y - H\tilde{x}) \tag{8}$$

Updated covariance

$$\hat{P} = (I - KH)\tilde{P} \tag{9}$$

Because of linearization, the deviations in position are the filter estimates that are added to the a priori values to obtain the new update. Treating the new update as a priori, Eqs. (4–9) are used to refine further. The filter equations are used in the factorization form using the *U-D* factorization techniques.[6]

State and Covariance Propagation Model

One very important aspect in using the sequential filter is the propagation of state and the covariance between the measurement times. When the filter estimates the position in inertial frame, the propagation of the state and covariance is carried out by integrating the equations of motion due to the central force and the perturbations. This involves good numerical integration algorithm.

Since the geosynchronous satellite is nearly stationary in Greenwich frame, the position in Greenwich frame is defined as the parameters to be estimated. This has greatly simplified the state dynamics without sacrificing any accuracy. Thus, if $\bar{X}(t)$ is the geodetic position at t, then the predicted state $\tilde{x}(t_2)$ is the same as the last estimated state $\hat{x}(t^1)$, i.e.,

$$\tilde{X}(t_2) = \hat{X}(t_1) \tag{10}$$

It is shown later that this model together with the proper model for the covariance gives very good estimates. The covariance propagation is given by

$$\tilde{P}(t_2) = \hat{P}(t_1) \tag{11}$$

Simulation studies revealed that the aforementioned model causes divergence due to $\hat{P}$ becoming very small after each measurement set. This was solved by adding an error matrix Q (which is a diagonal matrix) to increase $\tilde{P}(t_2)$ in Eq. (11). Since $\hat{P}$ is available in the form of U, D factors, Q is added to $D(t_1)$ to increase $\tilde{P}(t_2)$ effectively.

Simulation Studies

Table 1 shows the simulation details carried out for two types of orbits: a nearly geostationary orbit, and an inclined drift orbit with an inclination of 1 deg as well as a drift rate of 0.3 deg/day. Using the simulated observations, the aspects studied are 1) effect of Q matrix on filter estimate, 2) effect of iterations, and 3) effect of data interval.

Discussion

1) To start with, the simulated observations of the nearly geostationary orbit were used with state and covariance propagation given by Eqs. (10) and (11). In the absence of Q, the filter starts diverging after some time. This is shown in Fig. 2, which gives the variation of absolute position difference with time.

2) In order to arrest the divergence, the predicted covariance [Eq. (11)] was intentionally increased, just before processing a new measurement set, by adding a diagonal error matrix Q, i.e.,

$$D(t_2) = D(t_1) + Q \tag{12}$$

It was found that with just $Q = I$ (i.e., 1 km^2 diagonal) the estimated position was closely following the actual state as shown in Fig. 2.

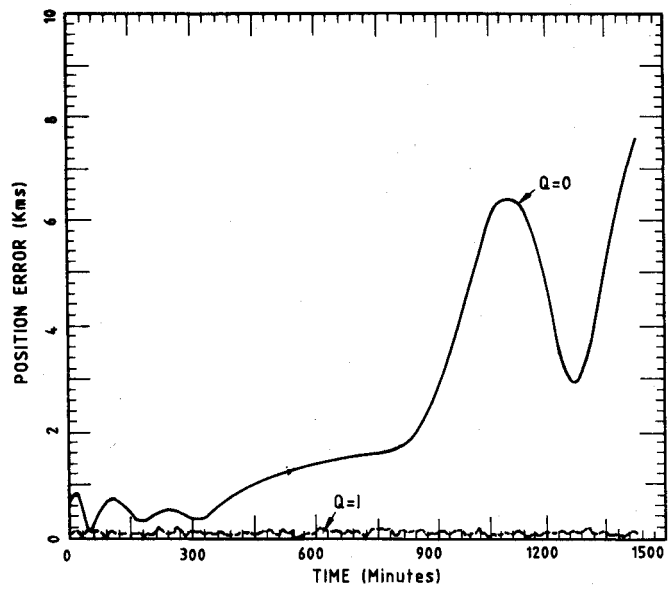

Fig. 2 Position error for nearly geostationary orbit with $Q=0$, $Q=I$.

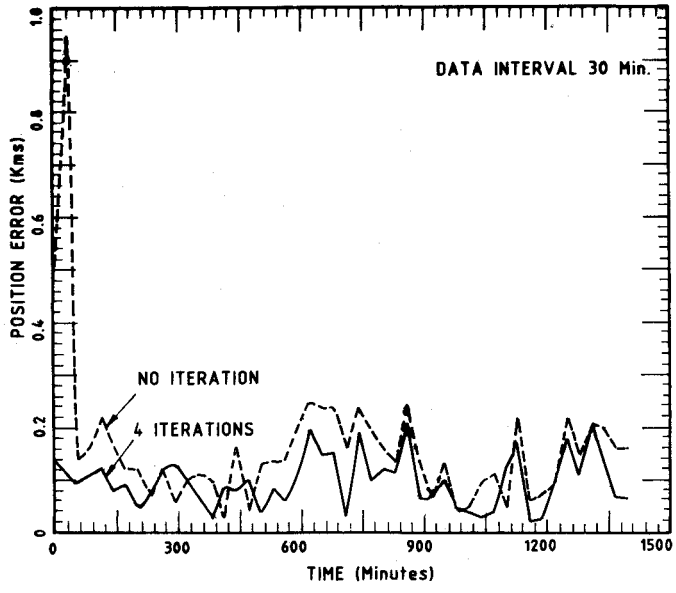

Fig. 3 Position eror for inclined drift orbit.

3) In the case of an inclined drift orbit, it was found that in addition to the Q matrix ($=I$), iterations were needed to bring down the measurement residues. With this strategy for four iterations and above, the measurement residue was almost zero. Figure 3 shows the position error variation in case of an inclined drift orbit.

Algorithm

Based on the analysis of the simulation results, the following algorithm is arrived at:

BEGIN
  INPUT a priori satellite position $\bar{X}_0$
  INPUT a priori covariance of position P_0
  Factorize P_0 into U, D factors
  $\hat{X}(t_1) := \bar{X}_0$
  WHILE observation is available DO
  BEGIN
    READ observation set ρ at $t = t_2$
    $\tilde{X}(t_2) := \hat{X}(t_1)$ [Eq. (10)]
    $\bar{X}(t_2) := \tilde{X}(t_2)$

```
    FOR iterations 1 to 4
      Compute observation set ρ_c using X̄(t_2)
      Δρ := ρ − ρ_c
      ∂ρ/∂X̄ := ρ̂^T
      Computation of estimated state X̂(t_2) and updating
      of U, D factors using UDU^T sequential estimation
      algorithm
      D := D + Q
      X̄(t_2) := X̂(t_2)
    NEXT ITERATION
    t_1 := t_2
    X̂(t_1) := X̂(t_2)
  END
END
```

Conclusion

By utilizing the range to three active landmarks, an estimation algorithm has been developed to estimate the geodetic satellite position. Simulation results showed that with such a simple model a position determination accuracy of better than 200 m can be achieved. The algorithm porposed is well suited for onboard applications because of its simplicity.

Acknowledgments

We thank Mr. K. N. Srinivasa Murthy for his fruitful suggestions in developing the algorithm, particularly in the area of inclusion of process noise in the estimation algorithm. Our thanks are also due to Mrs. B. P. Dakshayani for the help in providing the various types of simulated observations.

References

[1]Mease, K. D., Ryne, M. S., and Wood, L. J., "An Approach to Autonomous, Onboard Orbit Determination," AIAA Paper 84-2031, Aug. 1984.

[2]Liu, A. S., "Autonomous Satellite Navigation Using the Stellar Horizon Atmospheric Dispersion Sensor," AIAA Paper 83-861, Aug. 1983.

[3]Rene, Z. X., "Autonomous Satellite Navigation and Orbit-Keeping Using Attitude Sensors," IAF-ST-84-12, 35th Congress of the International Astronautical Federation, Lausanne, Switzerland, Oct. 1984.

[4]Hall, D. L. and Waligora, S. R., "Orbit/Attitude Estimation with Landsat 1 and 2 Landmark Data," AAS 79-152, *Astrodynamics 1979, Advances in Astronautical Sciences,* Vol. 40, Pt. 1, pp. 187–211.

[5]Chodas, P., "Application of Extended Kalman Filter to Several Formulations of Orbit Determination," Univ. of Toronto, Toronto, Ontario, Canada, UTIAS TN-224.

[6]Bierman, G. J., "Factorization Methods for Discrete Sequential Estimation," *Mathematics in Science and Engineering*, Vol. 128, Academic, New York, 1977, Chap 5.

Flexible Manipulator Modeling for Control System Development

V. A. Spector* and H. Flashner†
University of Southern California, Los Angeles, California

I. Introduction

WEIGHT limits imposed on space-based systems, such as robots, lead to highly flexible structures. Consequently, compensation for structural flexibility is an important factor in achieving performance specifications.[1-3] High-accuracy endpoint positioning requires direct measurement of end-effector position and possibly of displacements at intermediate locations, thus creating a noncollocated control system. Separating the actuators and sensors creates a delay between control action and sensors measurement, adversely affecting both system stability and performance. Propagation delay in flexible links has been experimentally found[4] to significantly limit control system performance.

In this Note, application of Euler and Timoshenko beam theories to flexible link modeling for control design is examined from several points of view. In addition to transfer functions (gain and phase), frequency-domain wave propagation solutions are obtained for both the Euler and Timoshenko models by using transform techniques. The resulting dispersion equations are analyzed to explain differences between the models and the impact of these differences on factors pertinent to control design, such as time delay. Bounds on the range of validity of Euler theory for control modeling are obtained by comparison of transfer functions with those resulting from Timoshenko theory.

II. Dynamic Equations of Motion

Consider the motion of a rotation beam undergoing a bending deformation $y(x,t)$ and a cross-sectional rotation $\psi(x,t)$. Assuming small motions, the resulting equations of motion are

$$EI\frac{A^2\psi}{\partial x^2} + \kappa GA\left(\frac{\partial y}{\partial x} - \psi\right) - \rho I\frac{\partial^2\psi}{\partial t^2} = 0 \tag{1a}$$

$$\rho A\frac{\partial^2 y}{\partial t^2} - \kappa GA\left(\frac{\partial^2 y}{\partial x} - \frac{\partial\psi}{\partial x}\right) = 0 \tag{1b}$$

where ρ is the mass density, A cross-sectional area, E the Young's modulus, G the shear modulus, κ the Timoshenko shear coefficient, and I the area moment of inertia.

Equations (1) represent the Timoshenko beam model.[5] This model includes both the rotary inertia and shear effects and is the most accurate model that derives from strength of materials. The shear coefficient κ is dimensionless and depends on Poisson's ratio and the shape of the cross section (see Ref. 6).

If both shear and rotary inertia are neglected, the Euler-Bernoulli model results:

$$EI\frac{\partial^4 y(x,t)}{\partial x^4} + \rho A\frac{\partial^2 y(x,t)}{\partial t^2} = 0 \tag{2}$$

III. Solution Methods

To solve the equations of motion, a Laplace transform with s as the time transform variable is taken. The resulting ordinary differential equation for the Laplace transform has the characteristic equation for the Euler-Bernoulli model:

$$p^4 + [(\rho A/EI)]/s^2 = 0 \tag{3}$$

and for the Timoshenko model:

$$p^4 - \frac{\rho}{E}s^2\left(1 + \frac{E}{\kappa G}\right)p^2 + \frac{\rho A}{EI}s^2\left(1 + \frac{\rho I s^2}{\kappa GA}\right) = 0 \tag{4}$$

The solution has the form

$$y(x,s) = \sum_{n=1}^{n=4} C_n(S)e^{p_n x} \tag{5}$$

where the characteristic exponents p_n, $n = 1,2,3,4$ are the roots of Eqs. (3) and (4), respectively. Explicitly, for the Euler-Bernoulli beam

$$p_{1,2} = \pm\left(-\frac{\rho A}{EI}\right)^{1/4} s^{1/2} \tag{6a}$$

Presented as Paper 87-2264, at the AIAA Guidance, Navigation, and Control Conference, Monterey, CA, Aug. 17-19, 1987; received Feb. 8, 1988; revision received June 6, 1988.

*Graduate Student, Department of Mechanical Engineering; currently, Senior Staff Engineer, TRW,

†Assistant Professor, Department of Mechanical Engineering. Member AIAA.